IFSCC 2025 full paper (IFSCC2025-1751)

Comprehensive Study on the Skin Care Efficacy of Heparin

Zheng Wang [1,*], Peixue Ling [1], Yumei Fan [1], Shuang Chen [1]

[1] Meyer Bio-medicine Co., Ltd., Shandong, China

Abstract

Heparin, a sulfated glycosaminoglycan traditionally used for its anticoagulant properties, has recently garnered interest in dermatology and cosmetic science due to its multifaceted bioactivities. This study investigates the potential skincare benefits of heparin, including antiaging, anti-inflammatory, antioxidant, skin repair and mitochondrial energy enhancement effects, through a combination of in vitro cell assays. Heparin sodium significantly induced the expression of elastin by 13.15% and inhibited the expression of MMP-1 by 22.58% in human primary dermal fibroblasts. Heparin sodium significantly inhibited the secretion of IL-1α cytokine and ROS production by 32.18% and 16.56% in human keratinocytes induced by UVB. Heparin sodium significantly increased the cell migration rate by 29.6% compared to control. Heparin sodium significantly increased the ATP production and mitochondrial membrane potential by 43.3% and 30.2% in human keratinocytes induced by UVB. These findings highlight heparin as a promising multifunctional ingredient for anti-aging, sensitive skin care, and barrier-enhancing cosmetic formulations. This study provides foundational evidence for the translational application of heparin in skincare products.

Keywords: Heparin; Antiaging; Anti-inflammation; Mitochondria; Skin repair

1. Introduction

Heparin, a naturally occurring polysaccharide first isolated from mammalian tissues in the early 20th century, has long been recognized for its anticoagulant properties in clinical medicine [1]. Beyond its hematological applications, emerging research suggests broader biological roles, including modulation of growth factors, inhibition of proteases, and regulation of inflammatory pathways [2,3]. Such diverse mechanisms have sparked interest in repurposing heparin for dermatological applications, particularly given its high biocompatibility and low immunogenicity [4].

Modern skincare science increasingly prioritizes ingredients with multifunctional efficacy to address complex concerns such as photoaging, chronic inflammation, oxidative stress, and compromised barrier function. While hyaluronic acid and peptides dominate current formulations, there remains a need for novel actives that simultaneously target multiple aging pathways. Heparin's unique molecular structure, characterized by sulfated glycosaminoglycan

chains, enables interactions with extracellular matrix proteins and cell surface receptors, suggesting untapped potential in modulating skin homeostasis [5]. Previous studies indicated heparin accelerates wound healing and exerts anti-inflammatory effects in burn models hint at utility for sensitive skin [6,7]. However, systematic evaluation of its cosmetic efficacy, particularly in comprehensive cell assays, remains lacking.

This study bridges this gap by comprehensively assessing heparin's skincare potential. We hypothesize that its dual anti-inflammatory and tissue-regenerative properties, combined with hydrophilic capacity, may synergistically improve skin firmness, hydration, barrier resilience, and photodamage repair. Using multiple in vitro cell assays, we evaluated its effects on key biomarkers and consumer-relevant endpoints. By elucidating molecular mechanisms and practical benefits, this work aims to establish heparin sodium as a scientifically validated cosmetic ingredient, offering formulators a novel tool to address multifactorial skin aging.

2. Materials and Methods

2.1 Reagents

Human primary dermal fibroblasts (HDFs) , human primary epidermal keratinocytes (NHEKs) and relevant culture medium were purchased from Lifeline® Cell Technology; Penicillin-Streptomycin-Amphotericin B solution was obtained from Bioind. DPBS was bought from Gibco; 6-well plates, 12-well plates, and 96-well cell culture plates were purchased from Thermo Fisher. Elastin ELISA Kit (Cat: HM11429) and MMP-1 ELISA Kit (Cat: HM10740) were supplied by Bioswamp. IL-1α ELISA kit was from R&D Systems (Cat. DY200). The Mitochondrial Membrane Potential Assay Kit was from Beyotime (Cat: C1073M) and the CellTiter-Glo® Luminescent Cell Viability Assay was from Promega (Cat: G7571). CellROX® Green Reagent was from Invitrogen™ (Cat: C10444).

2.2 Devices

Incubator (Thermo Fisher), inverted microscope (Leica), fluorescence microscope (Leica), biological safety cabinet (Thermo Fisher), microplate reader (Tecan), UVB lamp (Spectroline Model EB-160C).

2.3 Methods

2.3.1 MMP-1 ELISA Assay

When HDFs reached 80–90% confluence, they were trypsinized and seeded into 96-well plates. After 48 hours, the fibroblasts were starved overnight with serum-free starvation medium to synchronize the cell growth. Samples at different concentrations (N=3) were then prepared with starvation medium for cell treatment. After 48 hours, the supernatants were collected for MMP-1 ELISA testing according to the manufacture's instruction.

2.3.2 Elastin ELISA Assay

When HDFs reached 80–90% confluence, they were trypsinized and seeded into 96-well plates. After adherent culture for 48 hours, the fibroblasts were starved overnight with serum-free starvation medium to synchronize the cell growth. Samples at different concentrations (N=3) were then prepared with starvation medium for cell treatment. After 48 hours, the

supernatants were collected for elastin ELISA testing according to the manufacture's instruction.

2.3.3 IL-1α ELISA Assay

When NHEKs reached 80–90% confluence, they were trypsinized and seeded into 12-well plates. After 48 hours, cells were first treated with samples overnight, then induced for damage by UVB (35 mJ/cm²), and continuously treated with samples for an additional 24 hours. The supernatants were collected for IL-1α ELISA testing, according to the manufacture's instruction.

2.3.4 ROS generation

NHEKs were seeded in 96-well microplates at 2 × 104 cells/well for 48 h and then exposed to a spectral peak at 312 nm of the UVB irradiation by using an UVB lamp at doses of 10 mJ/cm2. After UVB irradiation, the cells were washed with warm DPBS, and then fresh medium with and without different concentrations of sample were added and incubated for 24 h. The relative levels of ROS were detected using CellROX® Reagent. Briefly, the cells were incubated with 5 μM CellROX® for 1 h and washed three times with PBS. ROS production was measured through the fluorescent intensity with the excitation and emission wavelengths set at 485 and 520 nm, respectively.

2.3.5 Scratch Assay

When HDFs reached 80–90% confluence, they were trypsinized and seeded into 6-well plates. After 48 hours until fully confluent, a 1000μL pipette tip was used to create a scratch in the central area of the cell monolayer. The wells were rinsed three times with DPBS to remove floating cell debris. Scratch images at 0 hour were captured using an inverted microscope, with 3 images taken per well. Sample was dissolved in culture medium to prepare sample solutions for cell treatment. TGF-β at 10 ng/mL was used as a positive control and each treatment group included 3 parallel wells. After 24 hours, healing images were captured at the same positions as the 0-hour scratch images. The Image J software was used to quantify the area of the wound region at 0 and 24 hours and calculate the wound healing rate of each group.

2.3.6 ATP Assay

When NHEKs reached 80–90% confluence, they were trypsinized and seeded into 96-well plates. After 48 hours, cells were first treated with samples overnight, then induced for damage by UVB (35 mJ/cm²), and continuously treated with samples for an additional 24 hours. ATP production in each group was detected according to the kit instructions.

2.3.7 Mitochondrial Membrane Potential Measurement

When NHEKs reached 80–90% confluence, they were trypsinized and seeded into 12-well plates. After 48 hours, cells were first treated with samples overnight, then induced for damage by UVB (35 mJ/cm²), and continuously treated with samples for an additional 24 hours. The culture medium was aspirated, and cells were washed once with DPBS. 200 μL of detection buffer was added according to the kit instructions, mixed gently, and incubated in the dark at room temperature (20–25°C) for 30 minutes. Fluorescence images were captured

using a fluorescence microscope, and quantitative analysis of fluorescence signals was performed using Image J.

2.3.8 Statistics

All results are presented as Mean±SD. Unpaired t-tests were used for comparing quantitative data, and a P-value <0.05 was considered statistically significant. In the figures, * denotes P<0.05, ** denotes P<0.01, and *** denotes P<0.001.

3. Results

3.1 Anti-aging effects

Figure 1 showed that 0.1% heparin sodium significantly inhibited the expression of MMP-1 by 22.58%, a key enzyme associated with collagen degradation [8], in human primary dermal fibroblasts. Figure 2 showed that 0.05% heparin sodium increased the synthesis of elastin by 13.15%, a critical structural protein for skin elasticity [9]. Both results showed that heparin sodium have excellent anti-aging effects.

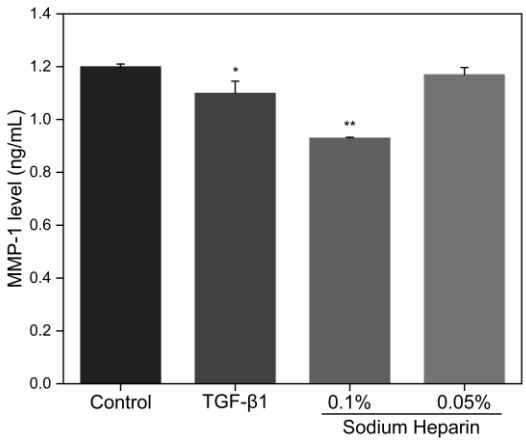

Figure 1. Effects of heparin sodium on the MMP-1 expression in dermal fibroblasts. For comparisons with the NC group, * signifies a p-value < 0.05, while ** signifies a p-value < 0.01.

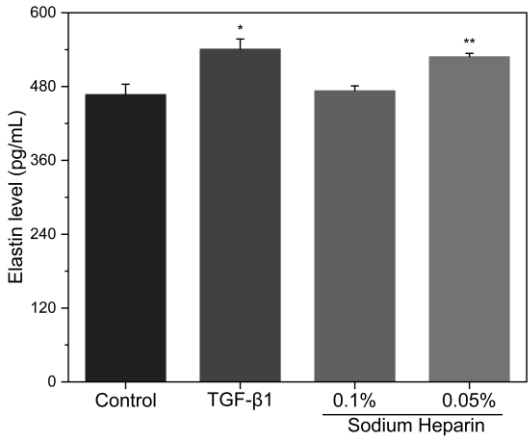

Figure 2. Effects of heparin sodium on the elastin expression in dermal fibroblasts. For comparisons with the NC group, * signifies a p-value < 0.05, while ** signifies a p-value < 0.01.

3.2 Anti-inflammatory effects

In keratinocytes, UV radiation causes cytokin IL-1α production, which is an important factor for skin inflammation [10]. To determine whether heparin sodium inhibits UVB-induced IL-1α synthesis in keratinocytes, we measured UVB induced IL-1α production of keratinocytes after heparin sodium treatment at 0.05% and 0.1%. Heparin sodium at 0.05% significantly inhibited IL-1α synthesis by 32.18% (Figure 3, $p < 0.05$). In addition, the inhibitory effect of heparin sodium on IL-1α synthesis is similar to that of vitamin C.

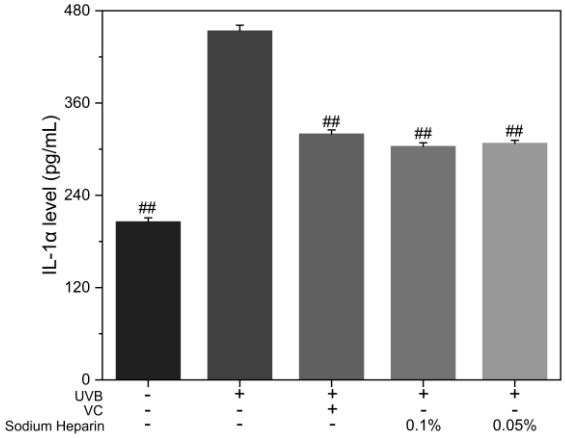

Figure 3. Effects of heparin sodium on IL-1α content in UVB-exposed keratinocytes. For comparisons with the BC group, # indicates a p-value < 0.05, and ## indicates a p-value < 0.01.

3.3 Antioxidant effects

To determine whether heparin sodium inhibits UVB-induced ROS production in keratinocytes, we measured UVB induced ROS production of keratinocytes after heparin

sodium treatment at 0.002%, 0.01% and 0.02%. Heparin sodium at 0.002% significantly inhibited ROS production by 16.56% (Figure 4, $p < 0.05$). In addition, the inhibitory effect of heparin sodium on ROS production is even better than that of vitamin C.

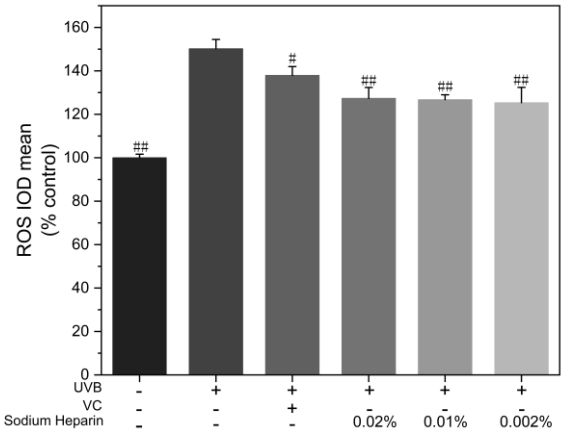

Figure 4. Effects of heparin sodium on ROS content in UVB-exposed keratinocytes. For comparisons with the BC group, # indicates a p-value < 0.05, and ## indicates a p-value < 0.01.

3.4 Skin repair effects

The in vitro scratch assay is particularly suitable for studies on cell migration, mimic cell migration during wound healing in vivo and are compatible with imaging of live cells during migration to monitor intracellular events if desired [11]. In the scratch assay, heparin sodium (0.2%) accelerated cells healing rate by 29.6% in human primary dermal fibroblasts compared to the control group at 24 hours as shown in Figure 5.

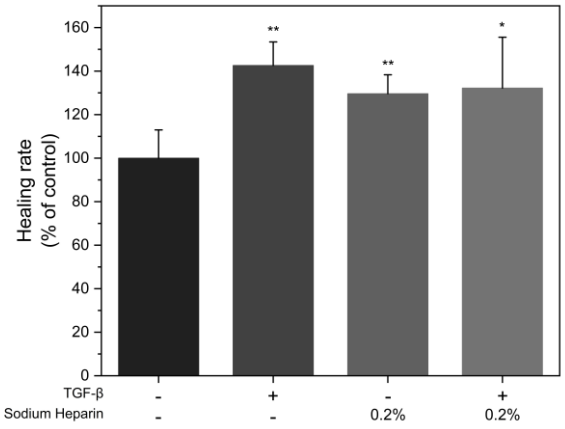

Figure 5. Effects of heparin sodium on the cells healing rate in dermal fibroblasts. For comparisons with the NC group, * signifies a p-value < 0.05, while ** signifies a p-value < 0.01.

3.5 Mitochondria function

The mitochondria are the primary organelle affected during chronological and UV-induced skin aging, the phenotypic manifestations of which are the direct consequence of mitochondrial dysfunction [12]. Heparin sodium attenuated UVB-induced mitochondrial dysfunction in human primary epidermal keratinocytes, as evidenced by its protective effects on ATP production and mitochondrial membrane potential, as shown in Figure 6 and Figure 7. Heparin sodium at 0.05% significantly induced ATP production by 43.3% and mitochondrial membrane potential by 30.2% (Figure 6 and 7).

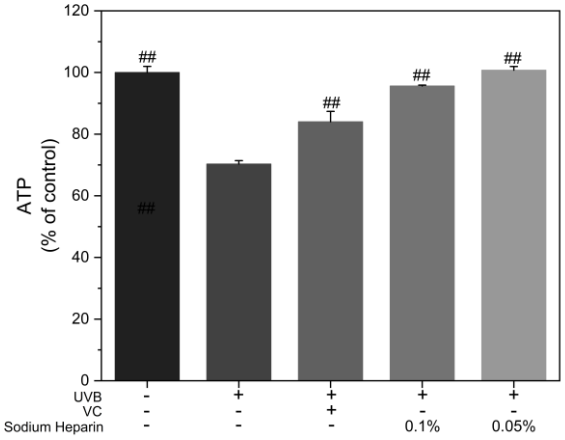

Figure 6. Effects of heparin sodium on ATP content in UVB-exposed keratinocytes. For comparisons with the BC group, # indicates a p-value < 0.05, and ## indicates a p-value < 0.01.

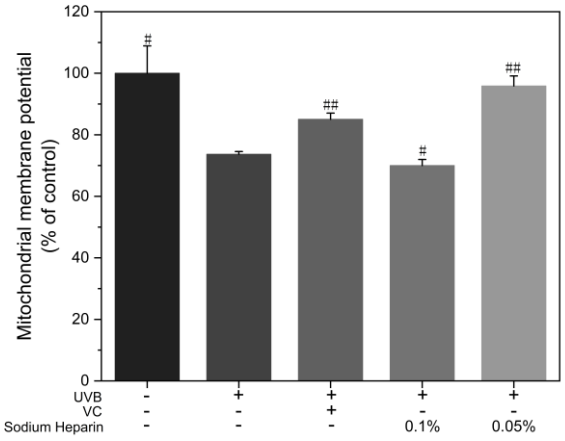

Figure 7. Effects of heparin sodium on Mitochondrial membrane potential content in UVB-exposed keratinocytes. For comparisons with the BC group, # indicates a p-value < 0.05, and ## indicates a p-value < 0.01.

4. Discussion

The findings of this study provide robust evidence supporting heparin sodium as a multifunctional bioactive agent with significant potential in skincare formulations. Its ability to

simultaneously inhibit MMP-1 (by 22.58%) and enhance elastin synthesis (by 13.15%) in human dermal fibroblasts underscores its anti-aging efficacy. By targeting collagen degradation and promoting structural protein synthesis, heparin sodium addresses two critical pathways in skin aging: extracellular matrix (ECM) remodeling and loss of elasticity. These effects align with previous studies demonstrating glycosaminoglycans' role in ECM stabilization, though heparin's sulfation pattern likely enhances its binding affinity to growth factors and protease inhibitors - amplifying its regulatory effects on fibroblast activity [13,14].

The anti-inflammatory properties of heparin sodium, evidenced by a 32.18% reduction in UVB-induced IL-1α secretion, further validate its utility in formulations targeting sensitive or photodamaged skin. This suppression of pro-inflammatory cytokine release may stem from heparin's ability to interfere with Toll-like receptor (TLR) signaling or sequester damage-associated molecular patterns (DAMPs), mechanisms previously implicated in its anti-inflammatory actions [15]. Notably, heparin's antioxidative capacity—reducing ROS by 16.56% in UVB-exposed keratinocytes—complements its anti-inflammatory effects, collectively mitigating oxidative stress and inflammation-driven skin damage.

Heparin sodium's promotion of wound healing (29.6% increase in migration rate) highlights its reparative potential. The synergy between heparin and TGF-β1 observed in scratch assays suggests heparin may act as a co-factor for growth factor stabilization, enhancing TGF-β1's bioactivity and fibroblast migration. This aligns with heparin's known role in facilitating growth factor-receptor interactions, a property leveraged in wound healing therapies [16].

Equally compelling are heparin's mitochondrial protective effects. By preserving ATP production and mitochondrial membrane potential in UVB-stressed keratinocytes, heparin sodium likely supports cellular energy homeostasis and barrier function. Mitochondrial dysfunction is a hallmark of photoaging, and heparin's ability to counteract UVB-induced damage positions it as a photoprotective agent [12]. These effects may be mediated through antioxidant mechanisms or direct stabilization of mitochondrial membranes, though further mechanistic studies are warranted.

While these in vitro results are promising, limitations must be acknowledged. The reliance on monolayer cell cultures may oversimplify the dynamic interactions within intact skin tissue. Additionally, the study focused on acute UVB exposure; long-term effects of heparin sodium on chronic photodamage remain unexplored. Future research should prioritize in vivo models to validate translatability, assess dose-response relationships, and investigate potential synergies with other anti-aging actives, such as retinoids or antioxidants.

5. Conclusion

In conclusion, this study demonstrates that heparin sodium exerts multifaceted skincare benefits, including anti-aging, anti-inflammatory, antioxidant, reparative, and mitochondrial-protective effects. By inhibiting MMP-1, promoting elastin synthesis, accelerating fibroblast migration, and mitigating UVB-induced oxidative and inflammatory damage, heparin sodium addresses key contributors to skin aging and barrier dysfunction. Its dual capacity to stabilize ECM components and enhance cellular resilience underscores its potential as a novel ingredient in anti-aging and photoprotective formulations.

These in vitro findings provide a scientific foundation for heparin sodium's inclusion in cosmetic products targeting multifactorial skin aging. However, clinical trials are essential to

confirm efficacy in human subjects, optimize concentrations, and evaluate long-term safety. Future investigations should also elucidate molecular mechanisms, such as heparin's interactions with growth factor signaling pathways or mitochondrial regulators. With further validation, heparin sodium could emerge as a cornerstone ingredient in next-generation skincare, offering holistic solutions for aging, sensitive, and environmentally stressed skin.

6. References

[1] Wang P, Chi L, Zhang Z, Zhao H, Zhang F, Linhardt RJ. Heparin: An old drug for new clinical applications. Carbohydr Polym. 2022 Nov 1;295:119818.

[2] Sasisekharan, R., Shriver, Z., Venkataraman, G., & Narayanasami, U. (2002). Roles of heparan-sulphate glycosaminoglycans in cancer. Science, 295(5564), 2379–2382.

[3] Taylor, K. R., Gallo, R. L., & Yamasaki, K. (2005). Heparin modulates the interaction of inflammatory cytokines with endothelial cells. Journal of Investigative Dermatology, 125(5), 923–929.

[4] Tykhomyrov, A. A., Pavlova, A. S., & Nedzvetsky, V. S. (2016). Heparin-induced modulation of oxidative stress in skin fibroblasts. Biochemistry Research International, 2016, Article 8196064.

[5] Sulfated polysaccharides in cosmetics: Heparin-like activity of glycosaminoglycans for skin barrier repair. Carbohydrate Polymers, 242, 116405.

[6] Saliba, M. J. (2001). Heparin in the treatment of burns: A review. Burns, 27(4), 349–358.

[7] Wang, L., Li, H., Zhang, Y., & Chen, X. (2019). Anti-inflammatory effects of heparin sodium in a murine model of ultraviolet B-induced skin photodamage. Journal of Dermatological Science, 94(3), 328–336.

[8] Feng C, Chen X, Yin X, Jiang Y, Zhao C. Matrix Metalloproteinases on Skin Photoaging. J Cosmet Dermatol. 2024 Dec;23(12):3847-3862.

[9] Weihermann AC, Lorencini M, Brohem CA, de Carvalho CM. Elastin structure and its involvement in skin photoageing. Int J Cosmet Sci. 2017 Jun;39(3):241-247.

[10] Montero P, Milara J, Pérez-Leal M, Estornut C, Roger I, Pérez-Fidalgo A, Sanz C, Cortijo J. Paclitaxel-Induced Epidermal Alterations: An In Vitro Preclinical Assessment in Primary Keratinocytes and in a 3D Epidermis Model. Int J Mol Sci. 2022 Jan 20;23(3):1142.

[11] Liang, CC., Park, A. & Guan, JL. In vitro scratch assay: a convenient and inexpensive method for analysis of cell migration in vitro. Nat Protoc 2, 329–333 (2007).

[12] Sreedhar A, Aguilera-Aguirre L, Singh KK. Mitochondria in skin health, aging, and disease. Cell Death Dis. 2020 Jun 9;11(6):444.

[13] Gandhi, N. S., & Mancera, R. L. (2008). The structure of glycosaminoglycans and their interactions with proteins. Chemical Biology & Drug Design, 72(6), 455-482.

[14] Tykesson, E., et al. (2018). Decoding the functions of glycosaminoglycan sulfation in extracellular matrix remodeling. Matrix Biology, 71-72, 112-127.

[15] Johnson, G. B., et al. (2020). Heparin inhibits TLR signaling by binding to DAMPs and blocking receptor interactions. Journal of Immunology, 204(3), 512-524.

[16] Sakiyama-Elbert, S. E. (2014). Heparin-binding delivery systems for growth factor stabilization in wound healing. Advanced Drug Delivery Reviews, 72, 176-187.